AJNR

Loculated intracranial leptomeningeal metastases: CT and MR characteristics.

Y Y Lee, R D Tien, J M Bruner, C A De Pena and P Van Tassel

AJNR Am J Neuroradiol 1989, 10 (6) 1171-1179
http://www.ajnr.org/content/10/6/1171

Loculated Intracranial Leptomeningeal Metastases: CT and MR Characteristics

Ya-Yen Lee[1]
Robert D. Tien[1,2]
Janet M. Bruner[3]
Charles A. De Pena[1]
Pamela Van Tassel[1]

Studies of twenty-five patients with loculated leptomeningeal tumor metastases diagnosed by CT and/or MR were analyzed retrospectively. Medulloblastoma was the most frequent primary tumor (8/25, 32%). Four subgroups of loculated patterns were identified. Type A included mass(es) limited to the subarachnoid space without obvious direct parenchymal infiltration; this pattern occurred in 12 patients, of whom five had associated diffuse pattern. Type B was characterized by mass(es) still predominantly in the subarachnoid space but with minor transpinal parenchymal infiltration; this pattern was found in five patients. Type C comprised subarachnoid mass(es) with marked transpinal extension mimicking parenchymal lesion; this pattern was observed in three patients. Type D consisted of subarachnoid mass(es) growing along the perineural CSF space; this pattern was noted in two patients. Additionally, two patients presented with combined A and C patterns, and one patient had a combined B and C pattern. More than half the patients (14/25, 56%) presented with a single lesion. The most frequent locations were the suprasellar cistern, ventricular walls, and lateral recesses of the fourth ventricle, Gd-DTPA–enhanced T1-weighted MR images appeared best for demonstrating the site and extent of disease.

Recognition of the loculated patterns of leptomeningeal metastases, which are less common than the diffuse pattern, is important to radiologists and clinicians for correct diagnosis and proper management of patients with this disease.

***AJNR* 10:1171–1179, November/December 1989; *AJR* 154: February 1990**

Leptomeningeal metastasis, previously known as meningeal carcinomatosis or carcinomatous meningitis, is a relatively uncommon mode of tumor spread. It may arise hematogenously through the meningeal vessels from the systemic neoplasms or from the shedding of tumor cells in certain primary CNS neoplasms. It often presents as diffuse or disseminated infiltration in the intracranial and intraspinal subarachnoid space. The intracranial abnormalities related to leptomeningeal metastasis on CT have been thoroughly described by Enzman et al. [1] and Lee et al. [2]. The four major CT abnormalities are (1) sulcal-cisternal enhancement, (2) ependymal enhancement, (3) widened irregular tentorial enhancement, and (4) communicating hydrocephalus.

Occasionally, collections of tumor cells can be loculated in the dependent or generous portions of the intracranial subarachnoid space, including the ventricles, forming a rather distinct extraaxial mass lesion. This phenomenon, when it occurs without diffuse pattern, may cause a diagnostic dilemma and delay proper management. Intracranial loculated leptomeningeal metastases, however, have never been well documented in the literature. The purpose of this retrospective study is to identify and categorize these less familiar patterns of leptomeningeal metastasis in order to improve diagnostic acumen and direct proper management.

Materials and Methods

Records of 25 cancer patients with leptomeningeal metastases manifested by loculated intracranial abnormalities on CT and/or MR were collected for this retrospective study. The

Received September 1, 1988; revision requested October 31, 1988; revision received April 11, 1989; accepted April 16, 1989.

[1] Department of Diagnostic Radiology, Division of Diagnostic Imaging, The University of Texas M.D. Anderson Cancer Center, 1515 Holcombe Blvd., Houston, TX 77030. Address reprint requests to Y-Y Lee.

[2] Department of Radiology, University of California, San Francisco, CA 94143.

[3] Department of Pathology, University of Texas M.D. Anderson Cancer Center, Houston, TX 77030.

0195-6108/89/1006–1171

diagnosis was confirmed by CSF cytology alone in 14 patients, by surgery alone in three patients, and by CSF cytology and surgery in two patients. Diagnosis in the remaining six patients was not confirmed histologically by CSF cytology, owing to the intracranial mass effect, nor by surgery. All 25 patients had CT studies on various scanners before and after IV contrast administration; the scan thickness varied from 5 mm to 10 mm. Twenty patients were studied by MR (the majority on a 1.5-T GE scanner). The MR technical parameters included slice thickness of 5 mm with a 1–2.5-mm interslice gap, 256 × 128 matrix, 24-cm field of view, and 2–4 excitations. Sagittal and axial scans were obtained in all patients, supplemented with coronal views in selected cases. Spin-echo pulse sequences with a long TR (2000) and short and long TEs (20/80) were obtained in addition to T1-weighted images (600–800/20–30). The most recent seven patients also had enhanced MR after IV administration of Gd-DTPA.

The size, site, and number of loculated leptomeningeal metastases were recorded. The CT attenuation coefficient of the lesions was compared with the normal cortex (i.e., hypodense, isodense, and hyperdense). The MR signal intensity was described as hyperintense, isotense, or hypointense relative to normal gray matter. The ability of each MR pulse sequence to characterize the lesions was assessed. When available, the CT and MR scans were compared.

TABLE 1: CT and MR Appearance of Loculated Leptomeningeal Metastases

CT	
Precontrast	Isodense or slightly hyperdense to CT attenuation of brain cortex
Postcontrast	Uniform and moderate-to-marked enhancement
MR	
T1-weighted pulse sequence	Hypointense or isointense relative to brain cortex and slightly hyperintense relative to CSF
Long TR, short TE pulse sequence	Hyperintense relative to surrounding CSF and isointense with brain cortex
T2-weighted pulse sequence	Isointense with surrounding CSF; occasionally less hyperintense than CSF
Enhanced T1-weighted sequence	Marked hyperintensity readily demarcated from normal brain and CSF

Results

The appearances of loculated leptomeningeal metastases are summarized in Table 1. All lesions were isodense or slightly hyperdense on the precontrast CT scans and had moderate to marked enhancement on postcontrast scans (Fig. 1). On the unenhanced MR studies, all lesions were hypointense or isointense on T1-weighted images and demonstrated brighter signal intensity than surrounding CSF and brain tissue on long TR/short TE images; the lesions often became obscured on T2-weighted images because of the hyperintensity of CSF (Fig. 2). Gd-DTPA–enhanced T1-weighted images were obtained in seven patients, and all showed marked enhancement of tumors (Figs. 2 and 3).

The size, number, and anatomic site of the loculated metastases as well as the primary tumors are detailed in Table 2. The most frequent underlying primary tumors were medulloblastoma (eight cases), malignant glioma (four cases), and squamous cell carcinoma of the lung (three cases). The size of the lesions varied from 5 mm to 8 cm in diameter. The configuration was often round or dome-shaped except when infiltrating into the perineural CSF space alongside a cranial nerve. The ependymal lesions tended to be small and multiple. The most frequent locations were the suprasellar cistern (eight cases), lateral ventricles (five cases), lateral recess of the fourth ventricle (five cases), cerebellopontine angle cistern (four cases), and fourth ventricle (three cases).

From the morphologic location of the loculated masses, four distinctive subgroups were identified as follows: type A, mass(es) limited to the subarachnoid space (Fig. 4); type B, subarachnoid mass(es) with minor parenchymal infiltration but without parenchymal edema (Fig. 5); type C, subarachnoid space mass(es) with edema (Fig. 6); and type D, mass(es) growing along the perineural CSF space and presenting as

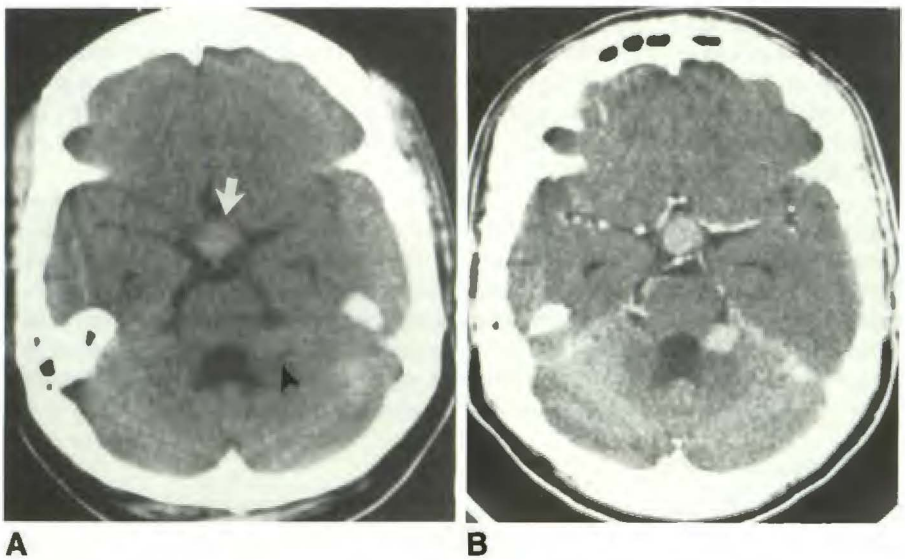

A B

Fig. 1.—Adenocarcinoma of breast.
***A*, Noncontrast CT scan. Suprasellar lesion is slightly hyperdense (*arrow*) and lesion in lateral recess of fourth ventricle appears isodense (*arrowhead*).**
***B*, Contrast-enhanced CT scan shows marked enhancement of both metastatic lesions.**

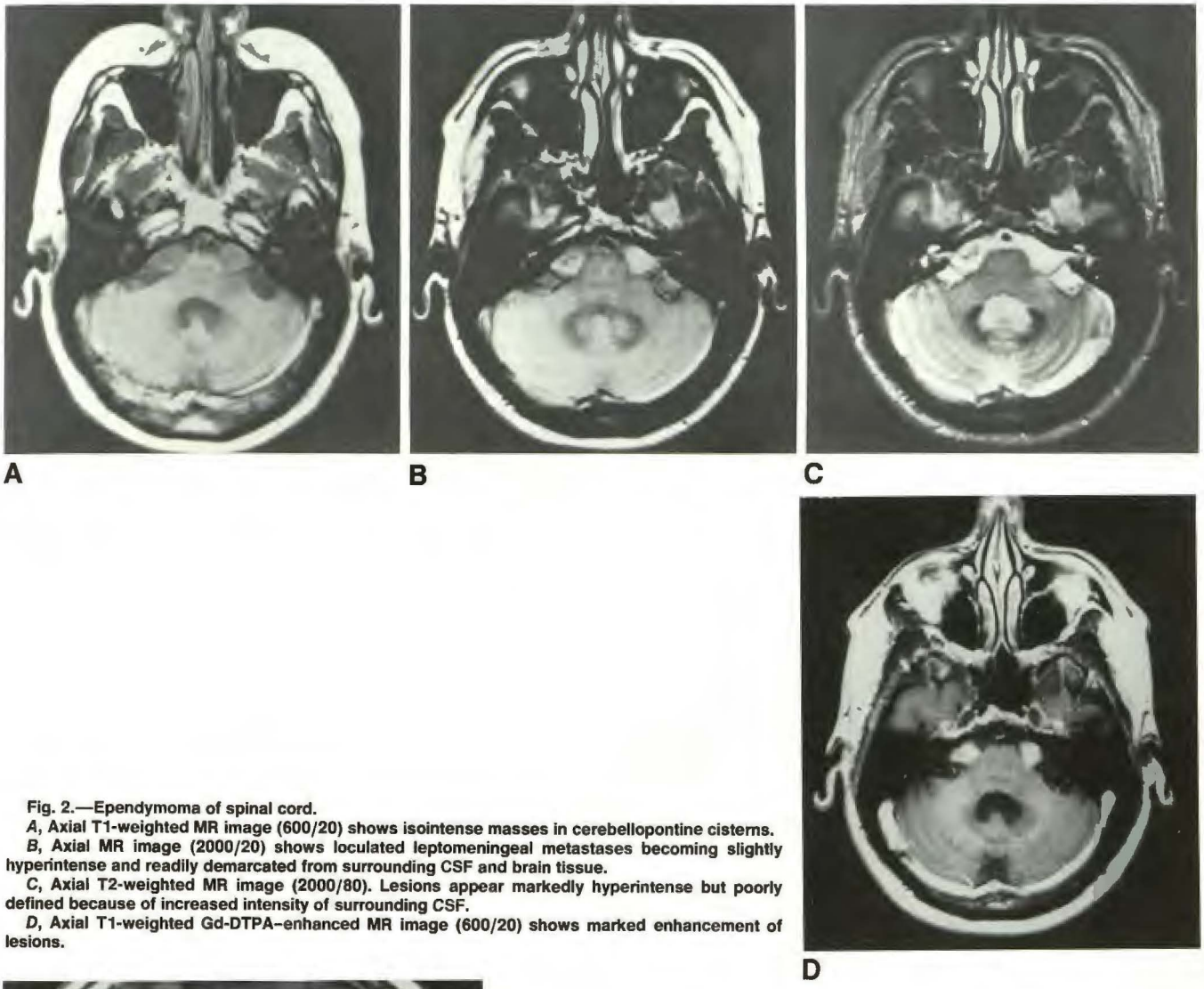

Fig. 2.—Ependymoma of spinal cord.
***A*, Axial T1-weighted MR image (600/20) shows isointense masses in cerebellopontine cisterns.**
***B*, Axial MR image (2000/20) shows loculated leptomeningeal metastases becoming slightly hyperintense and readily demarcated from surrounding CSF and brain tissue.**
***C*, Axial T2-weighted MR image (2000/80). Lesions appear markedly hyperintense but poorly defined because of increased intensity of surrounding CSF.**
***D*, Axial T1-weighted Gd-DTPA–enhanced MR image (600/20) shows marked enhancement of lesions.**

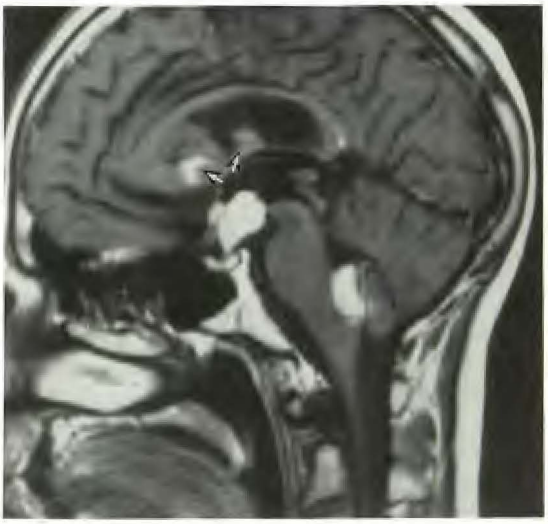

Fig. 3.—Medulloblastoma. Sagittal T1-weighted Gd-DTPA–enhanced MR image (600/20) shows marked enhancement of recurrent tumor within fourth ventricle and a large loculated leptomeningeal metastasis in suprasellar cistern infiltrating into hypothalamus. Also noted are less enhanced ependymal metastases (*arrows*).

extradural or extracranial lesion(s) (Fig. 7). The type A pattern, observed in 12 patients, was the most frequent. Five of these 12 also had a diffuse pattern of leptomeningeal metastasis. Type B was seen in five patients, and type C in three. Two cases of type D were identified. Two patients presented with combined types A and C, and one patient had combined types B and C.

Contrast-enhanced CT was better than unenhanced MR in defining the location and extent of loculated leptomeningeal metastases in all cases (Fig. 8). However, in the seven cases in which comparisons were available, Gd-DTPA–enhanced T1-weighted MR was far superior to contrast-enhanced CT in demonstrating the loculated lesions and in detecting additional subtle diffuse leptomeningeal metastases (Fig. 9).

Discussion

Leptomeningeal metastasis tends to be diffuse in both the intracranial and intraspinal subarachnoid spaces. Intracranially, the lesions are often more severe in the dependent

TABLE 2: Classification of Loculated Leptomeningeal Metastasis ($n = 21$)

Pattern	No. of Cases	Primary Tumor	Findings	Associated Diffuse Pattern	Pathologic Confirmation
A	12	1. Ependymoma of spinal cord	Bilateral 1.5-cm cerebellopontine angle cisternal masses, and one 3-cm suprasellar mass	No	None
		2. Squamous cell carcinoma of lung	3-cm mass in lateral recess of 4th ventricle	No	CSF
		3. Adenocarcinoma of breast	1-cm masses in suprasellar, superior cerebellar cisterns and lateral recess of 4th ventricle	No	CSF
		4. Medulloblastoma	1-cm mass in lateral recess of 4th ventricle	Yes	CSF
		5. Medulloblastoma	1.5-cm mass in lateral recess of 4th ventricle	Yes	CSF
		6. Squamous cell carcinoma of lung	2-cm mass in 4th ventricle	Yes	CSF
		7. Glioblastoma multiform of spinal cord	1.5-cm mass in suprasellar cistern	Yes	None
		8. Glioblastoma multiform	3-cm cerebellopontine angle mass	No	None
		9. Renal cell carcinoma	3-cm mass in subarachnoid space of posterior fossa	No	Surgery
		10. Anaplastic astrocytoma	1-cm masses in suprasellar cistern and 4th ventricle	Yes	CSF
		11. Oat cell carcinoma of lung	1-cm mass in left sylvian fissure	No	CSF
		12. Medulloblastoma	2-cm suprasellar mass and two 1-cm masses in lateral recess of 4th ventricle, and one 1-cm mass in cerebellopontine angle cistern	No	CSF
B	5	1. Medulloblastoma	6-cm suprasellar mass extending into hypothalamus and corpus callosum	No	None
		2. Squamous cell carcinoma of lung	Multiple ependymal-subependymal nodules (<1 cm) in lateral ventricles	No	CSF
		3. Anaplastic astrocytoma	Multiple cortical and ependymal-subependymal nodules in lateral ventricles	No	CSF

Table 2 continues

TABLE 2—*Continued*

Pattern	No. of Cases	Primary Tumor	Findings	Associated Diffuse Pattern	Pathologic Confirmation
		4. Medulloblastoma	3-cm suprasellar mass extending into hypothalamus and multiple ependymal-subependymal nodules in lateral ventricles	No	None
		5. Medulloblastoma	3-cm suprasellar mass extending into hypothalamus	No	Surgery
C	3	1. Medulloblastoma	4-cm mass on floor of right middle cranial fossa with edema	No	Surgery
		2. Medulloblastoma	6-cm bifrontal mass with edema	No	Surgery
		3. Lymphoma	Bilateral 1-cm temporal masses with edema	No	CSF
D	2	1. Leukemia	Dumbbell mass involving optic chiasm and right optic nerve	No	CSF
		2. Lymphoma	Dumbbell prepontine mass with involvement of Meckel cave and 5th cranial nerve	No	CSF & surgery
A & C	2	1. Germinoma	Small suprasellar and 4th ventricular masses and frontal horn subependymal mass with edema	No	CSF & surgery
		2. Melanoma	Ependymal nodules in lateral ventricle and 3-cm subependymal mass with edema	No	None
B & C	1	1. Lymphoma	1-cm ependymal mass and 2.5-cm subependymal mass with edema	No	CSF

portions of the cranial fossae or in areas where there are abundant CSF collections, such as the suprasellar cisterns, the cerebellopontine angle cisterns, and the ventricles. Microscopically, the tumor cells infiltrate the leptomeninges as a single layer or as thicker, multilayered aggregates. The earliest infiltration is along cortical vessels and is limited to the perivascular Virchow-Robin spaces. There is no transgression of the pia [3]. Most of these lesions are too small to be detected by currently available radiologic imaging techniques. When the tumor cells form larger aggregates, they may appear as a plaquelike coating on the surface of the brain, in the cisterns and fissures, along the tentorium, and/or on the ependymal lining of the ventricles. They can then be detected with contrast-enhanced CT [1, 2].

Occasionally, a mass of tumor accumulates in certain dependent locations where there is widening of the subarachnoid space. A subarachnoid extraaxial mass subsequently forms (type A) (Fig. 10). Further tumor growth leads to incursion into the underlying brain parenchyma while the main bulk of tumor remains in the subarachnoid space. At this stage the borders between loculated subarachnoid tumor and parenchymal infiltration become indistinct (type B) (Fig. 11). However, the degree of parenchymal infiltration is not severe enough to cause significant vasogenic edema in the brain

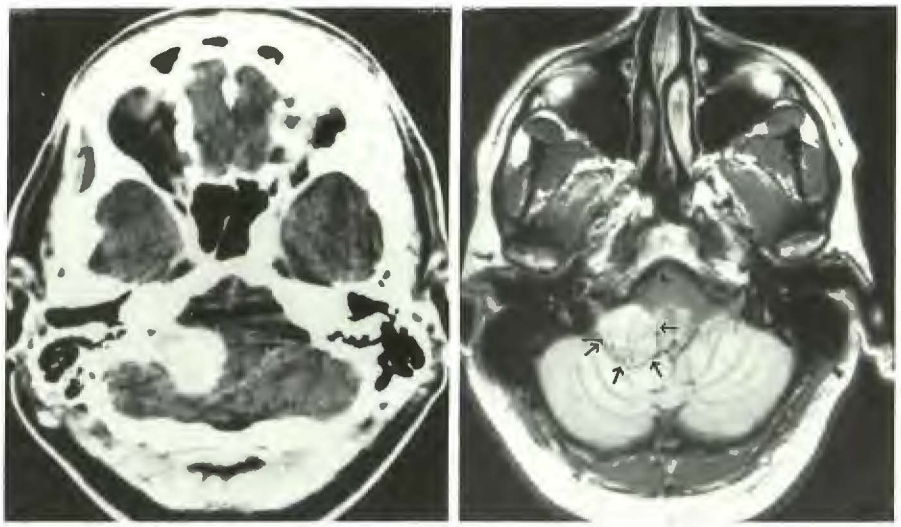

A B

Fig. 4.—Type A loculated leptomeningeal metastasis. Renal cell carcinoma.
A, Contrast CT scan shows markedly enhanced mass in region of right cerebellar hemisphere.
B, MR image (2000/20) shows slightly hyperintense extraaxial mass sharply demarcated from compressed inferior cerebellar hemisphere and medulla oblongata (*arrows*). Surgery confirmed metastatic tumor in subarachnoid space without parenchymal extension.

Fig. 5.—Type B loculated leptomeningeal metastasis. Medulloblastoma. Sagittal T1-weighted MR image (600/20) shows large suprasellar loculated metastasis infiltrating hypothalamus, third ventricle, and corpus callosum. Recurrent tumor is identified in fourth ventricle (*arrow*).

A B

Fig. 6.—Type C loculated leptomeningeal metastasis. Medulloblastoma.
A, Noncontrast CT scan shows multilobulated bifrontal isodense mass with extensive parenchymal edema.
B, Contrast-enhanced CT scan shows marked and solid enhancement of this infiltrating metastasis. Note enhanced falx (*arrows*) within tumor. Surgery revealed large subarachnoid metastasis with extensive transpinal infiltration.

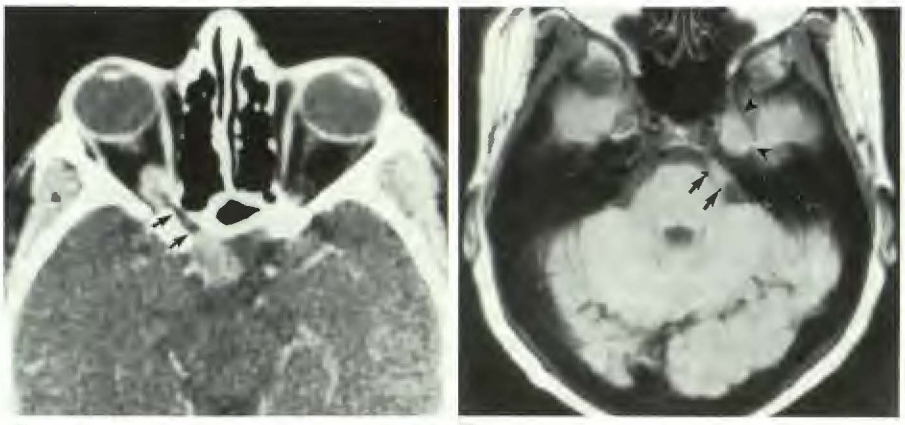

A B

Fig. 7.—Type D loculated leptomeningeal metastasis. Diagnosis proved by CSF cytology.
A, Contrast-enhanced CT scan shows acute lymphocytic leukemia. Dumbbell enhanced mass is growing along right optic nerve. Note normal optic canal (*arrows*).
B, MR image (200/20) shows diffuse large-cell lymphoma. Dumbbell mass is growing along left trigeminal nerve (*arrows*) into gasserian ganglion (*arrowheads*). Diagnosis proved by positive CSF cytology and open biopsy of gasserian ganglion.

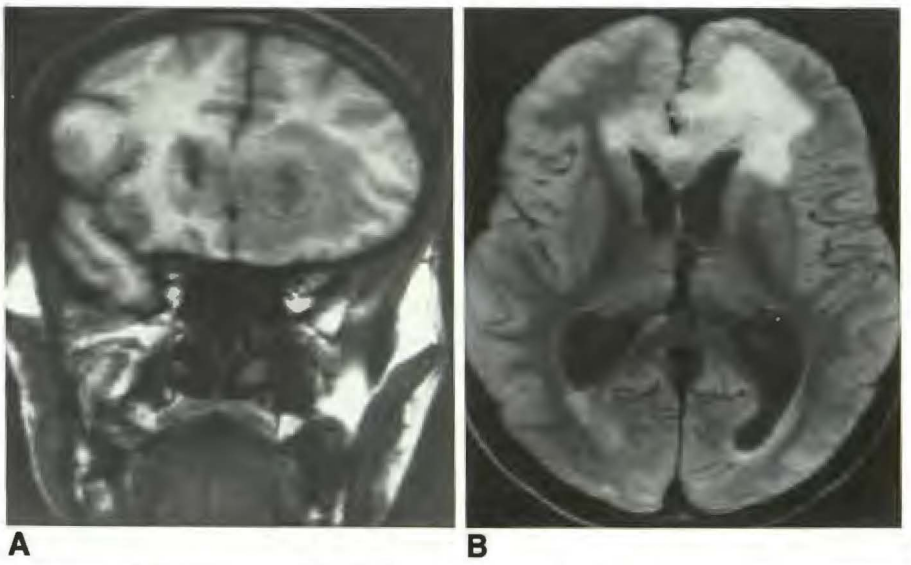

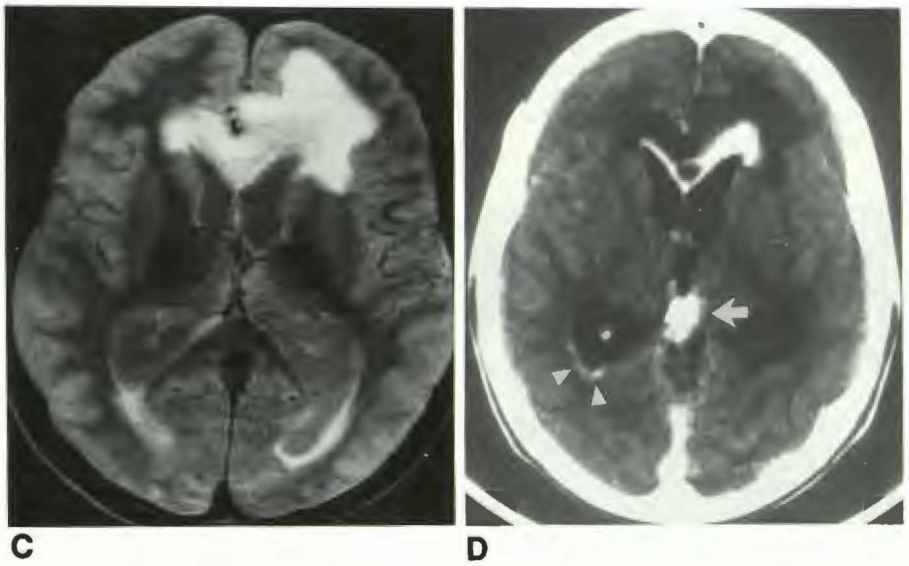

Fig. 8.—Pineal germinoma.

***A–C*, Coronal T1-weighted MR image (500/30) (*A*) and axial MR images, (2000/30) (*B*) and (2000/60) (*C*), show bifrontal periventricular abnormal intensities, more severe on left, with effacement of frontal horns. The lesion is not well defined.**

***D*, Contrast-enhanced CT scan. Metastatic lesion is markedly enhanced and sharply demarcated from associated parenchymal edema (type C). Recurrent tumor is identified in heavily calcified pineal gland (*arrow*). Also noted is minimal ependymal metastasis in right occipital horn (*arrowheads*).**

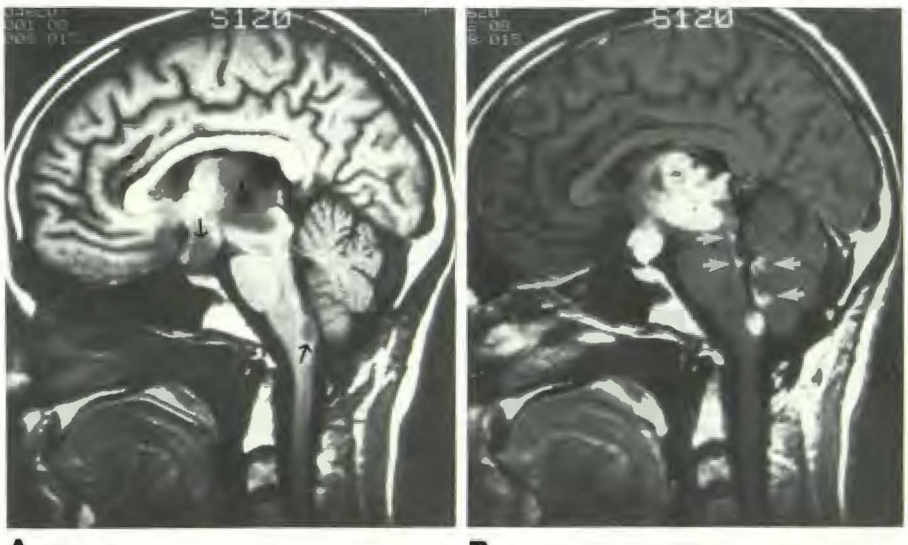

Fig. 9.—Anaplastic astrocytoma of thalamus.

***A*, Unenhanced sagittal T1-weighted MR image (600/20) shows hypointense recurrent tumor (*asterisk*) and loculated leptomeningeal metastases in suprasellar cistern and fourth ventricle (*arrows*).**

***B*, Gd-DTPA–enhanced sagittal T1-weighted MR image (600/20) shows marked enhancement of tumors, which are now better defined. Additional plaquelike enhancements of diffuse leptomeningeal metastases are noted (*arrows*).**

Fig. 10.—Loculated leptomeningeal metastatic melanoma without invasion of underlying brain cortex. There is no histologic evidence of brain edema or reaction. (Empty spaces are artifactual, caused by tissue detachment at time of cutting section.) (H and E, ×80)

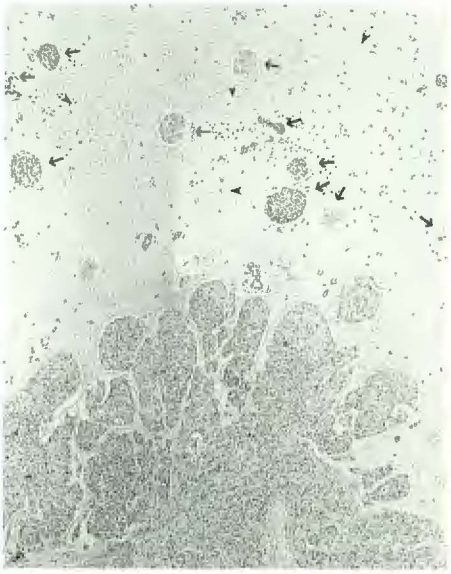

Fig. 11.—Loculated leptomeningeal metastatic breast carcinoma with invasion of superficial cortex and extension into Virchow-Robin spaces (*arrows*) in deep cortex. Small vacuoles of edema are present (*arrowheads*). (H and E, ×80)

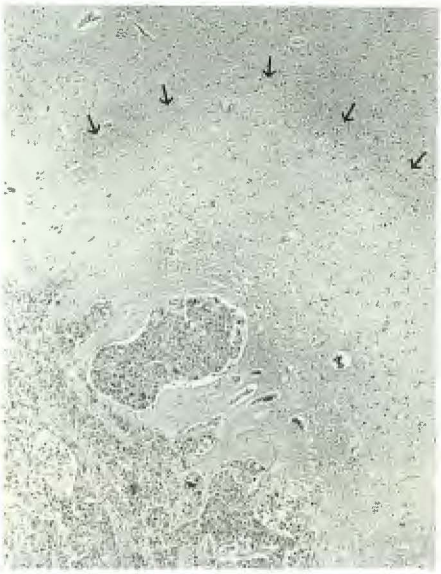

Fig. 12.—Further cortical invasion of loculated leptomeningeal metastatic breast carcinoma. A distinct pale area of cerebral edema surrounds the invasive carcinoma, rimmed by small vacuoles (*arrows*). (H and E, ×80)

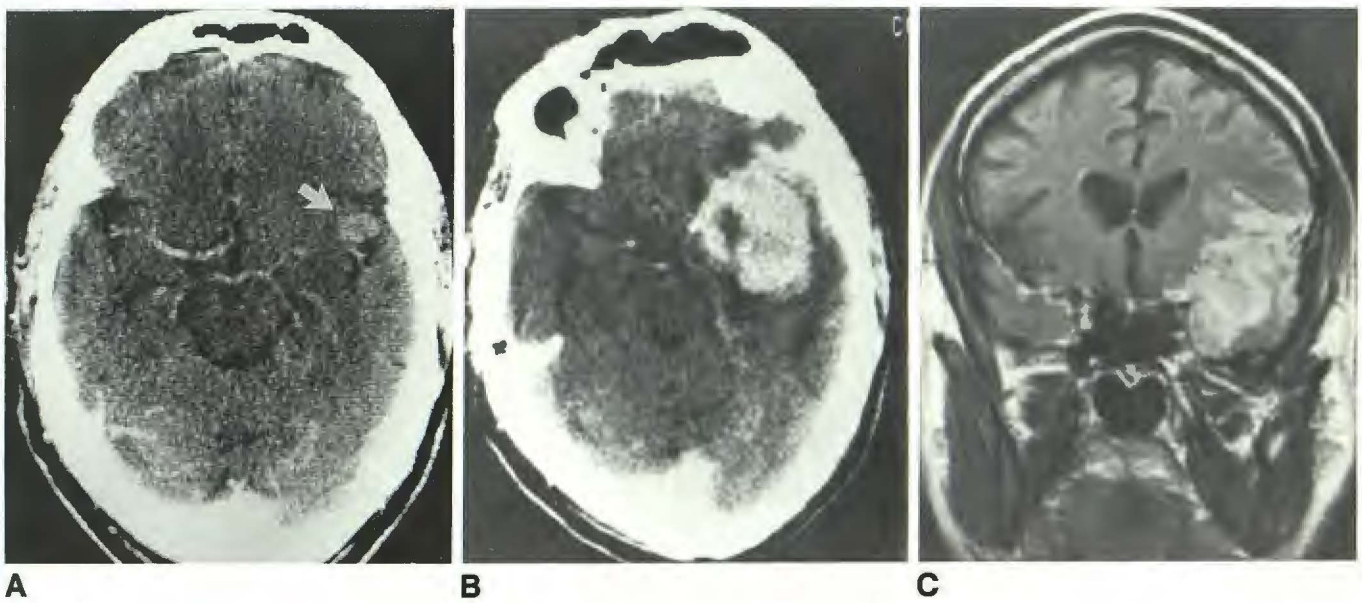

Fig. 13.—Oat cell carcinoma of lung.
A, Contrast-enhanced CT scan shows 1-cm loculated subarachnoid metastasis (type A) in left sylvian fissure (*arrow*). Positive CSF cytology.
B, Contrast-enhanced CT scan 7 months later. Lesion has progressed and associated with vasogenic edema (type C), mimicking parenchymal lesion.
C, Coronal Gd-DTPA–enhanced T1-weighted MR image (600/30) better demonstrates tumor growth along sylvian fissure into brain parenchyma.

parenchyma. When parenchymal infiltration becomes extensive and spreads farther away from the pial surface, the tumor loses its distinct extraaxial character and mimics a parenchymal tumor, particularly in the presence of associated parenchymal vasogenic edema (type C) (Figs. 12 and 13). The most unusual loculated proliferation of leptomeningeal metastases is characterized by tumor cells trapped and growing in the invaginated subarachnoid space accompanying the cranial nerve(s) (type D). Further outgrowth of tumor may extend under the Schwann cell sheath of cranial nerves into the extradural space. This appearance may be misdiagnosed as cranial nerve neurilemoma (schwannoma). The lesion may also mimic an optic glioma if the optic nerve is involved. This rare type of loculated leptomeningeal metastases had been

noted at autopsy [4] but has not been documented in the radiologic literature [5, 6].

The loculated patterns of leptomeningeal metastasis are often observed as isolated lesions. In our series, only five (20%) of 25 cases were seen with diffuse leptomeningeal metastasis. Not infrequently, the loculated leptomeningeal metastasis was present as a single lesion (14/25, 56%). However, ependymal lesions along the ventricular wall tend to be multiple.

Abnormal leptomeningeal contrast enhancement is nonspecific for leptomeningeal metastases and results from any entity causing blood-meningeal barrier abnormalities or increased leptomeningeal vascularity [7–9]. It can be appreciated on both CT and MR. However, in animal studies, MR has been more revealing than CT [8]. Our study indicates that multiplanar MR is far superior to CT, not only in delineating the exact location and extent of the loculated leptomeningeal metastases but also in detecting small plaquelike seedings undetected by CT. Gd-DTPA–enhanced T1-weighted MR appears to be the method of choice for imaging both loculated and diffuse leptomeningeal metastases.

REFERENCES

1. Enzmann DR, Krikorian CY, Haywood R. Computed tomography in leptomeningeal spread of tumor. *J Comput Assist Tomogr* **1978**;2:448–455
2. Lee Y-Y, Glass JP, Geoffrey A, Wallace S. Cranial computed tomography (CCT) abnormalities in leptomeningeal metastasis. *AJNR* **1984**;5:599–563
3. Ascherl GF, Hilal SK, Brisman R. CT of CSF dissemination of malignant neoplasms. In: Wood JH, ed. *Neurobiology of CSF*. New York: Plenum, **1983**:427–439
4. Mirfakhraee M, Crofford MJ, Guinto FC Jr, Nauta HJW, Weed VW. Virchow-Robin space: path of spread in neurosarcoidosis. *Radiology* **1986**; 158:714–720
5. Terry TI, Dunphy EB. Metastatic carcinoma in both optic nerves simulating retrobulbar neuritis. *Arch Ophthalmol* **1933**;10:611–614
6. Yuh WTC, Wright DC, Barloon TJ, Schultz DH, Sato Y, Cervantes CA. MR imaging of primary tumors of trigeminal nerve and Meckel's cave. *AJNR* **1988**;9:665–670
7. Sze G, Abramson A, Krol G, et al. Gadolinium-DPTA in the evaluation of intradural extramedullary spinal disease. *AJNR* **1988**;9:153–163
8. Frank JA, Girton M, Dwyer AJ, Wright DC, Cohen PJ, Doppman JL. Meningeal carcinomatosis in the VX2 rabbit tumor model: detection with GD-DTPA–enhanced MR imaging. *Radiology* **1988**;167:825–829
9. Mathews VP, Kuharik MA, Edwards MK, D'Amour PG, Azzarelli B, Dressen RG. Gd-DTPA–enhanced MR imaging of experimental bacterial meningitis: evaluation and comparison with CT. *AJNR* **1988**;9:1045–1050